CHAPTER V

RESULTS AND DISCUSSIONS

This chapter is separated into 4 sections. The first section reports the results of the NCL#1. Effect of cooling system on single-phase natural circulation is presented and temperature oscillation of water is also discussed. The next section reports the results of the NCL#2. The third section of this chapter presents the results from computer simulation. The results from computer program are compared with the experimental data and will be presented in the final section.

5.1 The results of the NCL#1

5.1.1 Effect of cooling system on single-phase natural circulation

The water temperature measured across the heater and the cooler at 473 W heating powers when the cooling system was turned off and turned on are as shown in Fig. 5.1 and Fig. 5.2, respectively. It should be noted that the time required to reach the steady state was decreased with the cooling system turning on.

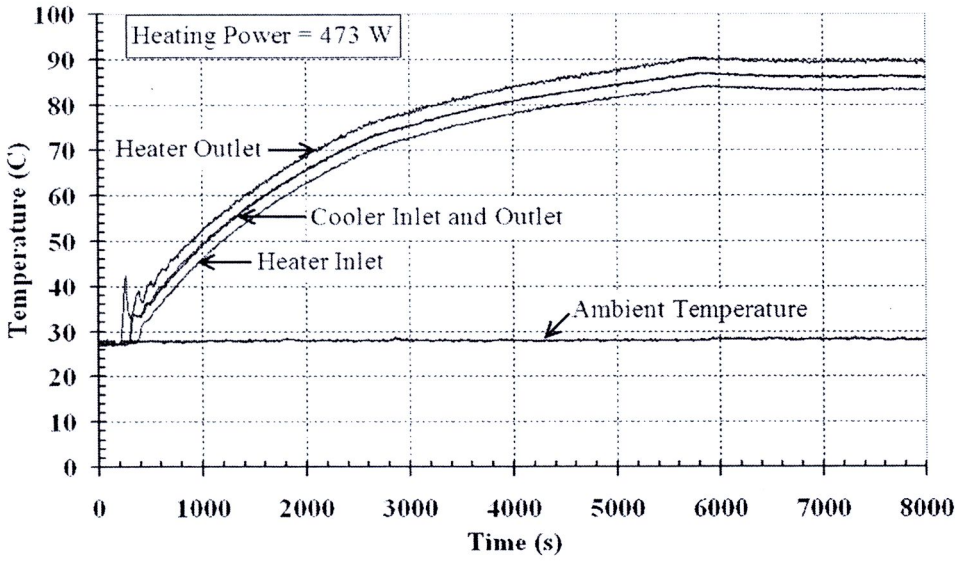

Fig. 5.1 The water temperature at 473 W heating powers when the cooling system was turned off

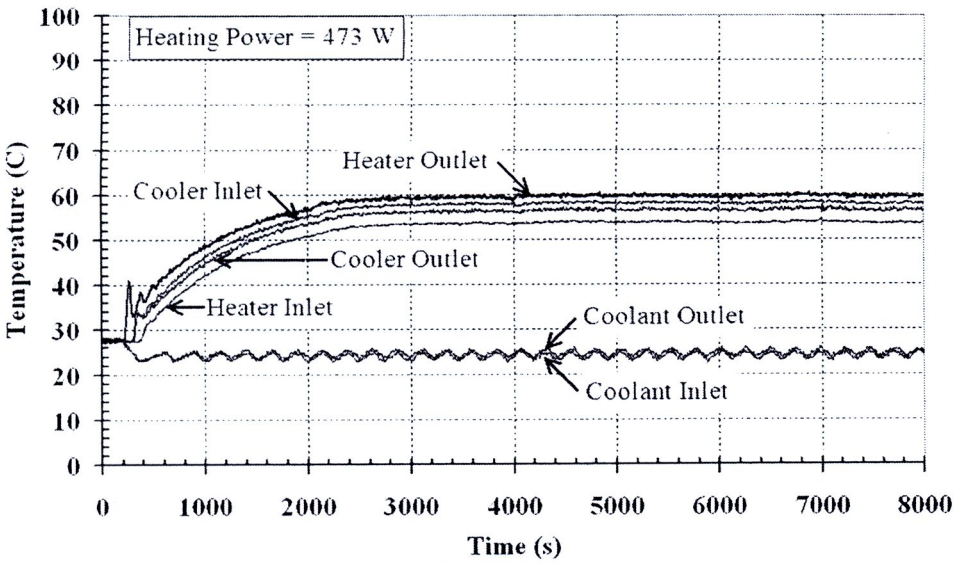

Fig. 5.2 The water temperature at 473 W heating powers when the cooling system was turned on

Maximum temperatures at the heater outlet for different heating power levels are as shown in Fig. 5.3. It was found that the maximum temperature was increased with the increasing heating power. In addition, for the same heating power, the maximum temperature was much higher when the cooling system was turned off compared with that obtained when the cooling system was turned on. It should be noted that the heating power level was limited to 473 W because the maximum temperature in the heating section was already very close to the saturating temperature for the water at atmospheric pressure.

Fig. 5.4 shows the temperature differences across the heater for different heating power levels with the cooling system turning off and turning on. It was found that at any given time the temperature difference only was slightly increased with the increasing heating power. The same behaviors for temperature differences were observed regardless of the turning condition of the cooling system.

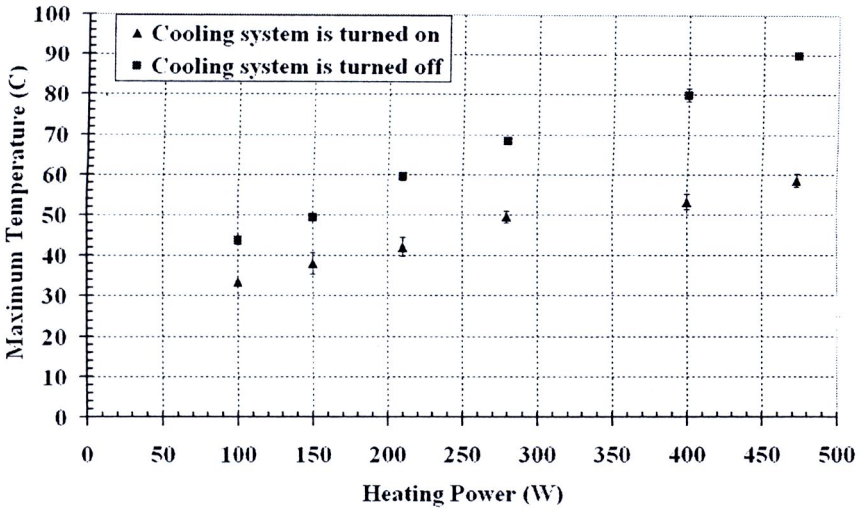

Fig. 5.3 The maximum temperature at the outlet heater for the different heating power levels

The maximum temperature at the heater outlet was found to depend on both the heating power level and the presence of the cooling system. However, the temperature difference across the heater was only affected by the heating power level. This was considered due to the limitation of the heater capacity. In effect the amount of heat received by the water flowing through the heater remained the same regardless of the inlet temperature.

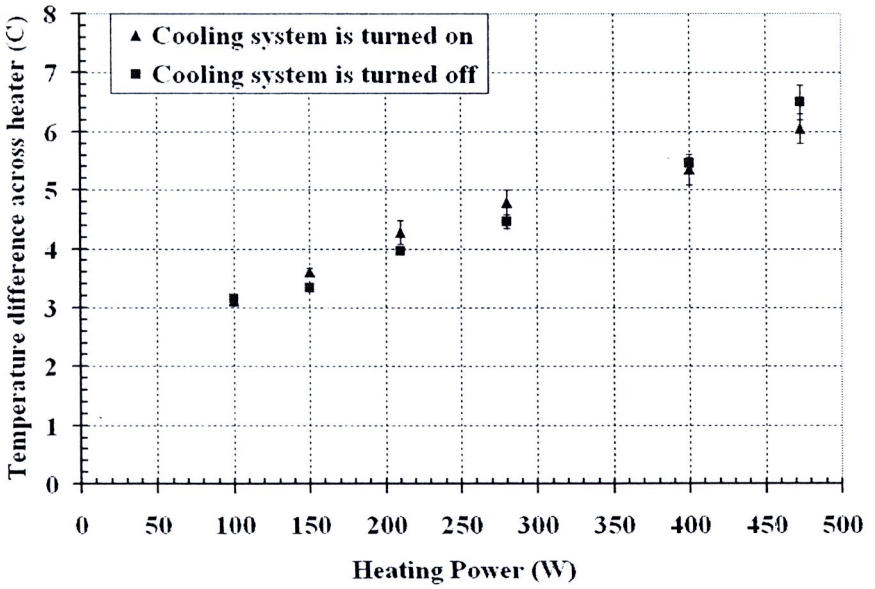

Fig. 5.4 Effect of heating power on the temperature difference across the heater

The mass flow rate due to the density gradient at the steady state was computed from the heating power and the temperature difference across the heater based on the conservation of energy. The macroscopic conservation of energy equation for a steady flow was expressed as

$$Q = \dot{m} C_p (T_o - T_i)$$

where T_i and T_o were respectively the mean fluid temperatures at the inlet and the outlet of the heating section, $\dot{m}$ was the mass flow rate, C_p was the specific heat capacity, and Q was the heating power. The value of C_p is temperature dependent. For this study, the value averaged from that at the inlet and the outlet is used. The values of mass flow rates computed at various heating power levels are as plotted in Fig. 5.5. The result indicated that the mass flow rate was increased with the increasing heating power. Again, the same mass flow rates were acquired regardless of the turning condition of the cooling system.

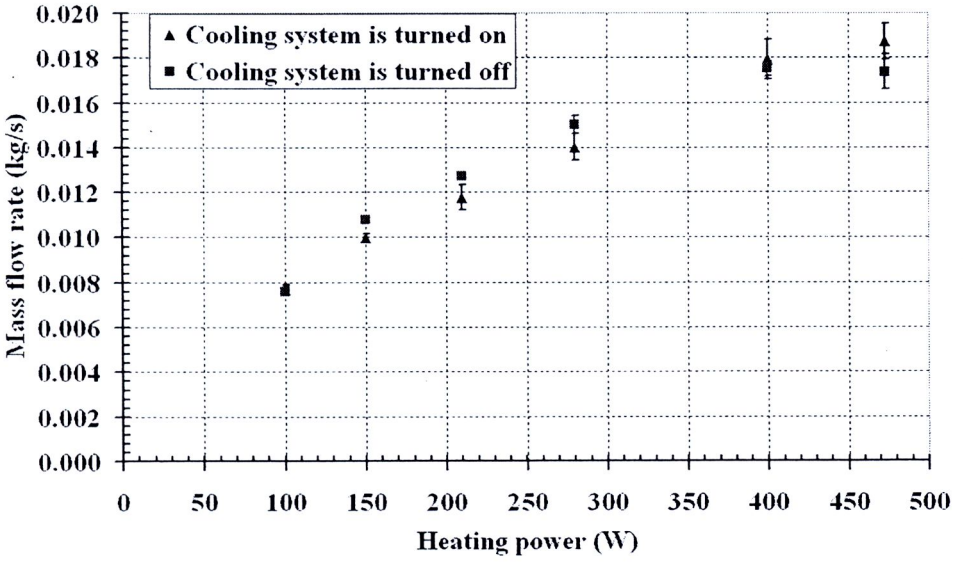

Fig. 5.5 Effect of heating power on the mass flow rates

4.1.2 The temperature oscillation

The water temperatures measured at the heater inlet and outlet at 575 W heating powers are as shown in Fig 5.6. The fluctuation is water temperature due to flow oscillation was observed during the starting of heater and after the water boiling. At the

water heater startup, the heater power was turned on but the water flow rate in the loop was essentially zero. As the water in the heating section absorbed heat from heater and caused the water temperature at the heater outlet to increase, the natural circulation was then initiated since the buoyancy force due to the density gradient had become greater than the overall friction in the loop. As the flow was established in the loop, the water temperature at the heater outlet would be decreased since the heating section was filled with colder water.

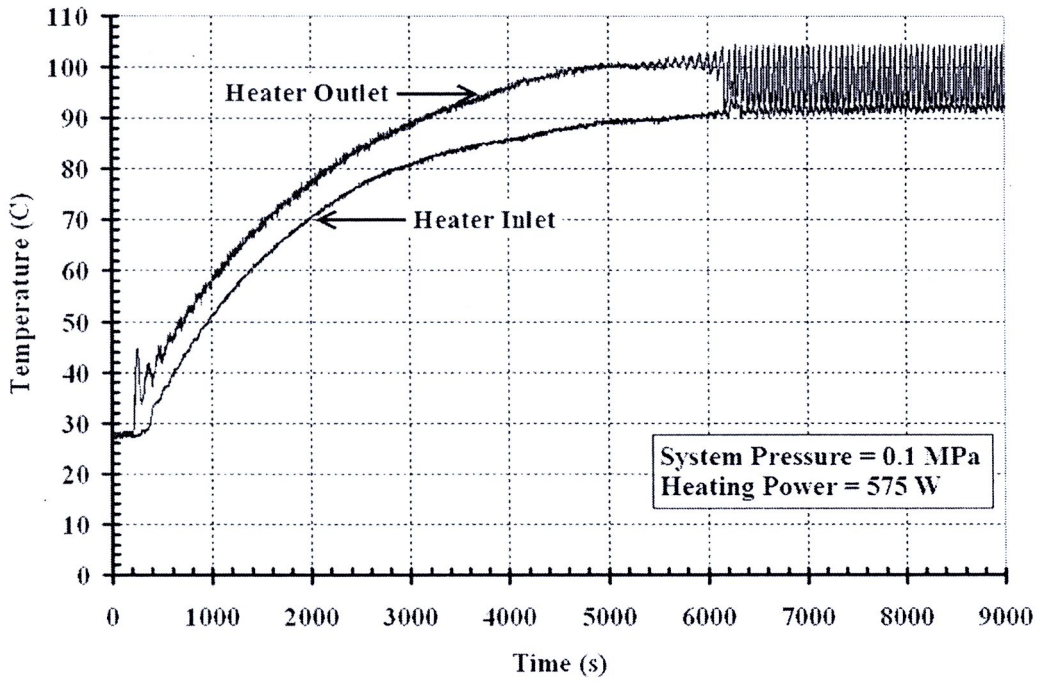

Fig. 5.6 The water temperature at the heater inlet and outlet of 575 W heating powers

As shown in Fig. 5.6, the water temperature at the heater outlet initially fluctuated wildly before it was settled down and began to gradually increase toward the boiling point. The amplitude of the initial fluctuation was found to increase as the heating power level was increased as show in Fig. 5.7. It should be noted that no boiling was observed for the heating power level that was less than or equal to 475 W.

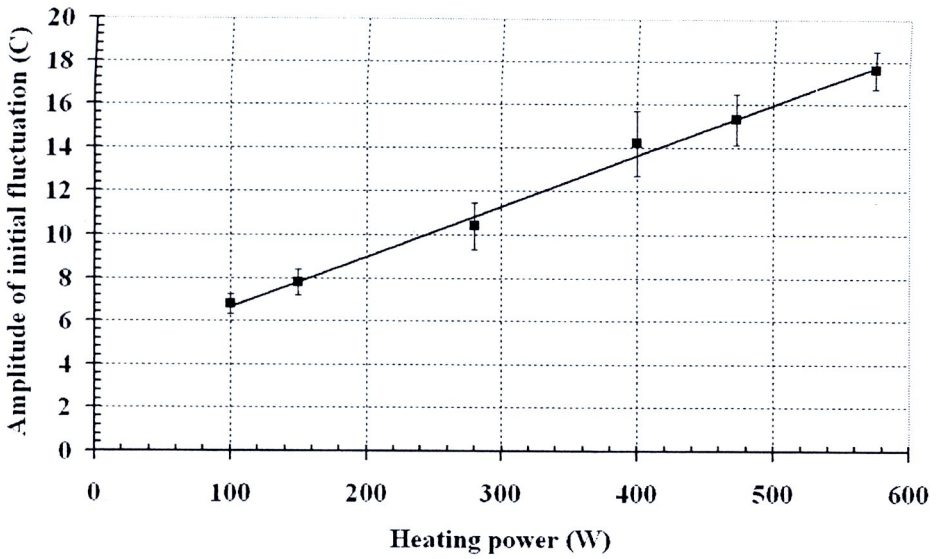

Fig. 5.7 The amplitude of initial fluctuation of the water temperature at the heater outlet

After the water boiling, the water began to boil more steam bubbles were produced and collected at the top horizontal tube. The process of the temperature oscillation at the heater outlet is as presented in Fig. 5.8. It could be described into 3 steps. In step 1, the collected steam was released from the expansion tank. At this point, two phenomena had been observed. First, the subcooled water flowed down the downcomer tube at the very fast speed. The heat was then transferred less effectively to the water because the water only spent a short amount of time in the heating section. This caused the boiling to stop. Second, the water from the expansion tank flowed in reverse direction to replace the void created by the release of the steam. When the two flows met, the net flow rate was decrease. In step 2, the water temperature was increased because the water was absorbed more heat due to stagnant flow and the boiling was re-started. In step 3, the steam bubbles were produced rapidly and rose again to the top without getting trapped in the top horizontal tube. The water temperature at the heater outlet was decreased rapidly due to the subcooled water flow down at high speed. The process then repeated again from step 1.

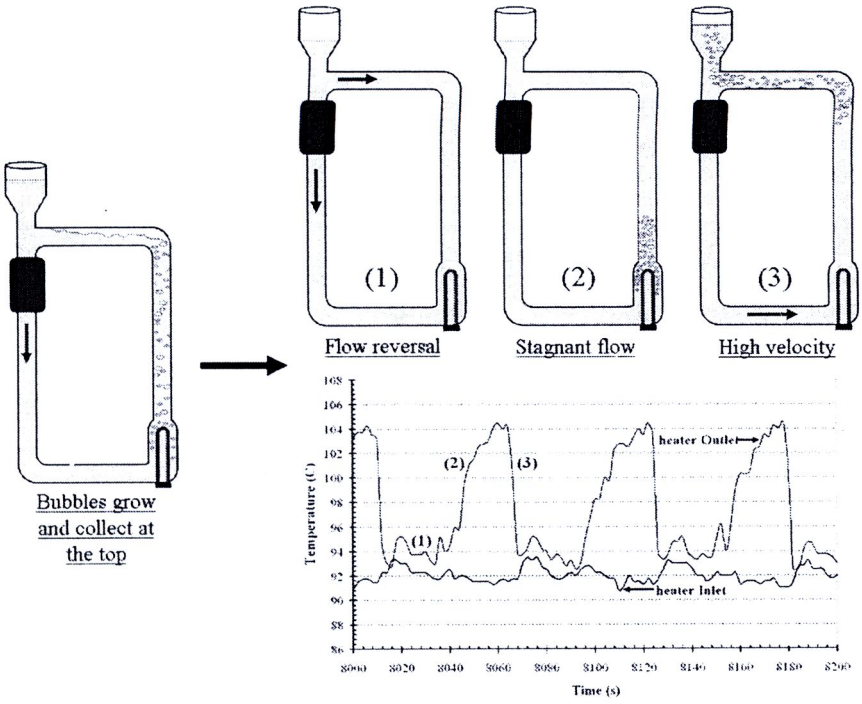

Fig. 5.8 The process of the water temperature oscillation after the water boiling

FFT method was used to analyze the water temperature oscillation at the heater outlet. FFT profiles of the water temperature oscillation at 575 W and 630 W heating powers are as shown in Fig. 5.9 and Fig. 5.10, respectively. The main frequency was found to be 0.02 Hz for 575 W heating powers. At 630 W heating powers, the main frequency was 0.025 Hz. The re-started boiling time in step 2 of the process of the water temperature oscillation was decreased when the heating power levels was increased. It should be noted that some of the hot water spilled during the boiling instability at 630 W heating powers.

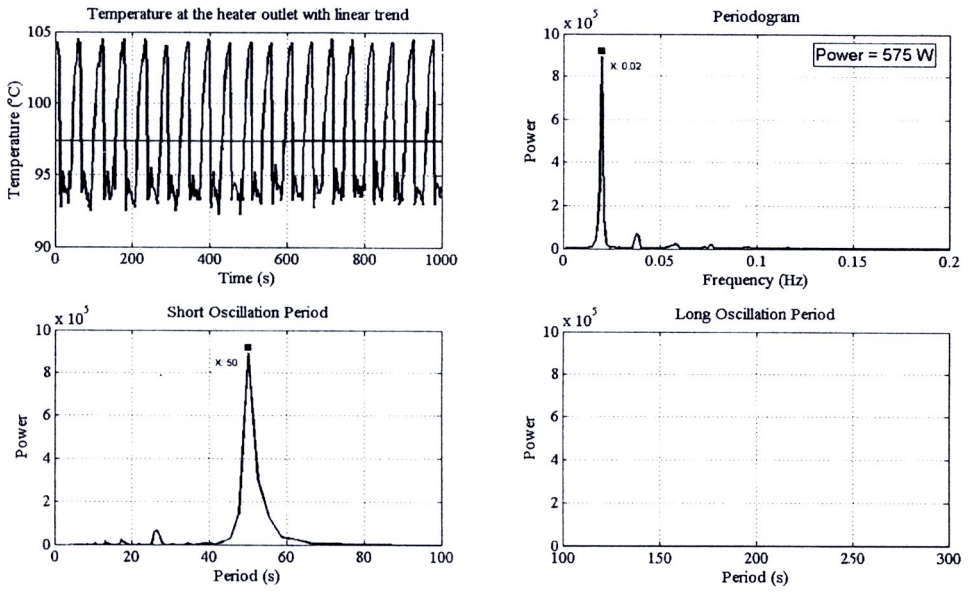

Fig. 5.9 FFT profile of the temperature oscillation at 575 W heating powers

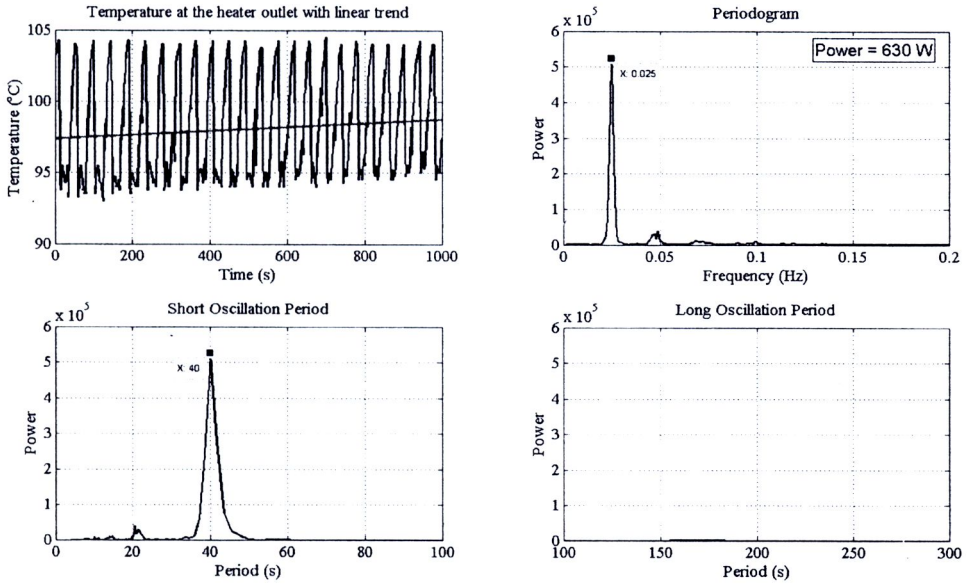

Fig. 5.10 FFT profile of the temperature oscillation at 630 W heating powers

From the result of this work, it was speculated that the temperature oscillation of water in this configuration was due to the presence of the horizontal tube. In order to minimize the oscillation in the two-phase flow caused by this configuration, the horizontal tube should be minimized or eliminated.

5.2 The results of the NCL#2

Fig. 5.11 and 5.12, show respectively the temperature profiles and the differential pressure across the heater at various heat flux levels: 6.0, 8.0, 12.5, and 18.0 kW/m^2. Each graph in Fig. 5.11 shows the temperatures at the heater inlet and outlet, and at the condenser inlet and outlet. Note that the time scale in each graph is not the same as boiling occurs faster at higher heat flux. As shown in Fig. 5.11(a), the temperature oscillation is not observed at all positions mention above. Fig. 5.11(b)-(d) shows the amplitude of temperature oscillation at the condenser outlet increased with increasing heat flux. The temperature oscillation at the heater outlet is due to the process of flashing-induced density wave oscillation, but the temperature oscillation at the condenser outlet is due to heated water flowing through the condenser. It should be note that flashing-induced density wave oscillation was observed when stable two-phase oscillation was occurred. At subcooled boiling start, geysering was observed at the riser. Process of geysering and flashing-induced density wave oscillation will be presented in the next section.

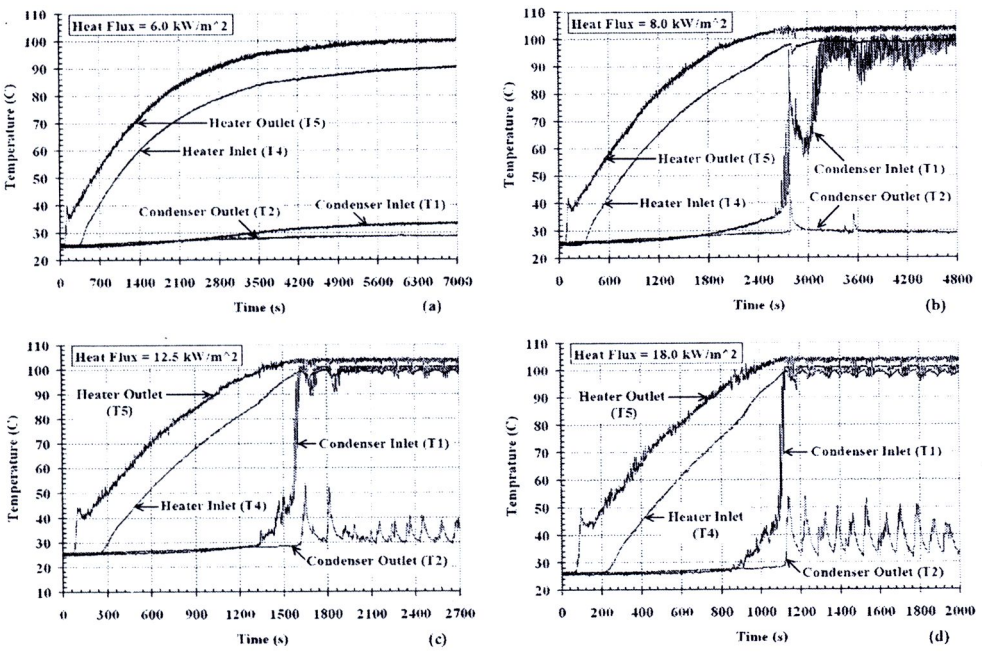

Fig. 5.11 The temperature profiles at various heat flux levels (a) 6.0 kW/m^2, (b) 8.0 kW/m^2, (c) 12.5 kW/m^2, and (d) 18.0 kW/m^2

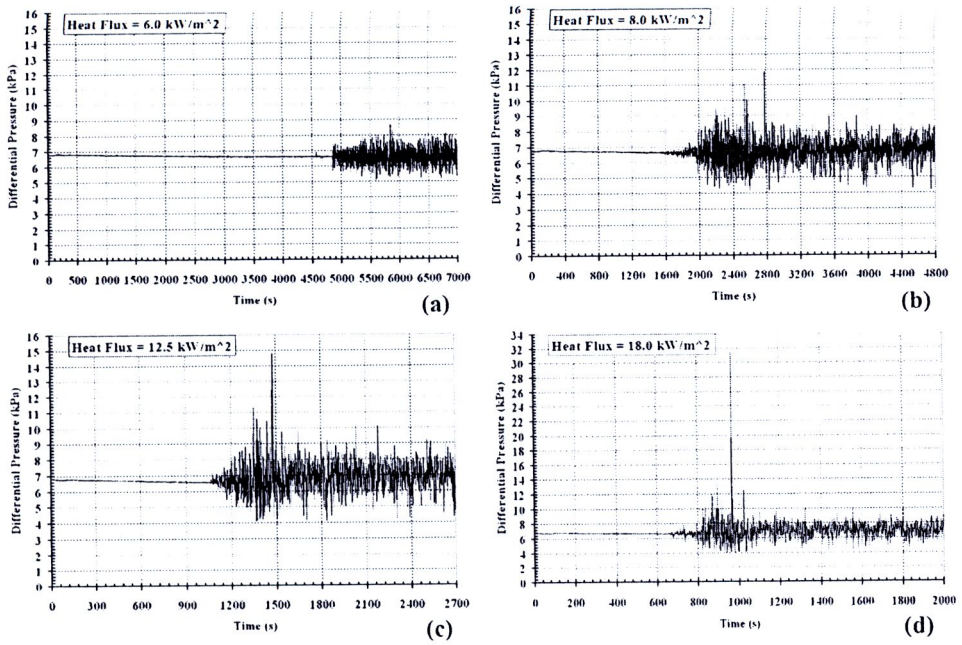

Fig. 5.12 The differential pressure across the heater at various heat flux levels (a) 6.0 kW/m^2, (b) 8.0 kW/m^2, (c) 12.5 kW/m^2, and (d) 18.0 kW/m^2

5.2.1 Geysering induced by condensation

As subcooled boiling occurs, bubbles departing from heater rod are condensed in subcooled water at the riser. In 1993, Aritomi et al. [8] observed the process of geysering in parallel boiling channels as shown in Fig. 5.13. Their proposed model for the driving mechanism of geysering is as follows:

> *"A large bubble covering the entire flow cross section is formed and grows towards the outlet plenum due to the decrease in hydrostatic head. As soon as the large bubble reaches the outlet plenum, it is mixed with subcooled water and condensed rapidly therein. Subcooled water reenters rapidly from the inlet plenum as the pressure drop corresponds to that in the other channel. If the condensation rate, that is, the reentering rate is higher than the circulation one, flow reversal is induced in the other channel. Both channels are filled with liquid and non-boiling condition is restored. After a while, a slug bubble is formed in the other channel because temperature of fluid reentering from the outlet plenum is higher than that in the channel. Such a process periodically repeats alternatively in both channels."[8]*

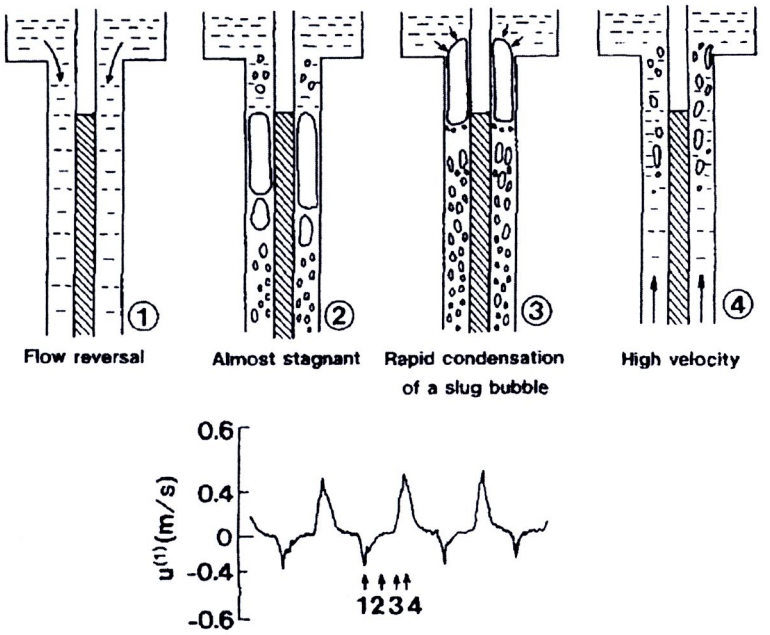

Fig. 5.13 Proposed model of geysering in parallel boiling channels [8]

Geysering was observed at the heater outlet for 8.0 heat flux as shown in Fig. 5.14. When subcooled boiling occurs at the heating section, a slug bubble is formed at the heater outlet. As the slug bubble enters to the riser, it is condensed with subcooled water. This process occurs until the water temperature in the riser reaches saturation point.

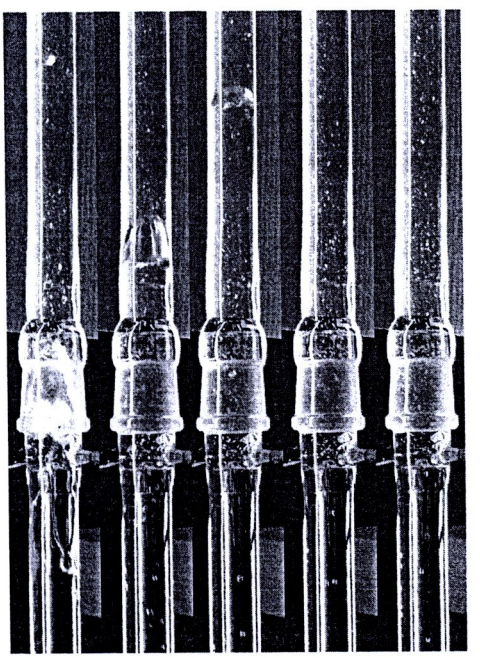

Fig. 5.14 Recorded bubble images at the heater outlet

5.2.2 Flashing-induced density wave oscillation

In 2005, Furuya et al. [11] presented process of flashing-induced density wave oscillation as shown in Fig. 5.15. They described it in the following steps:

"(a) Water heated by the heater (at 110 C for instance) flows into the chimney.

(b) Boiling initiates where the water temperature exceeds the local saturation temperature.

(c) Decrease in static head of water immediately promotes further evaporation, which is known as the flashing phenomenon.

(d) Natural circulation flow rate increases due to enlarged vapor volume resulting in outflow of the steam bubbles. In turn, the temperature at the chimney inlet becomes relatively low because of short dwell time in the heated region.

(e) After the chimney is filled with cold water, the flow rate decreases and the temperature at the chimney inlet becomes relatively high because of long dwell time in the heated region due to stagnant flow. The process repeats again from process (a)."[11]

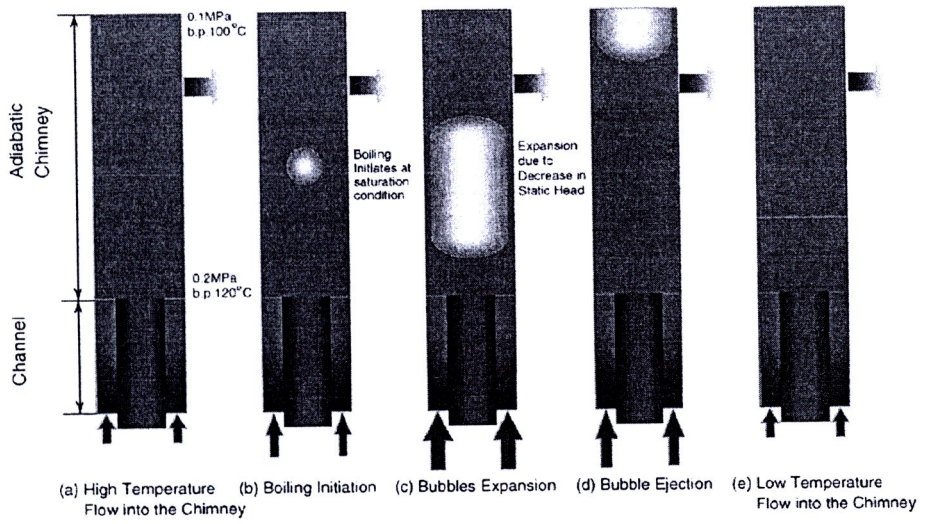

Fig. 5.15 Process of flashing-induced density wave oscillation [11]

Flashing-induced wave density oscillation was observed and bubble images were recorded at the riser middle for 8.0 heat flux as shown in Fig. 5.16. As can be observed, a slug bubble (t = 0 s) rises upward to the expansion tank and transfer heat to the water in the riser. When the water temperature exceeds the saturation point, it starts to boil (t = 1 s). In t = 1-4 s, Bubbles expand due to decrease in static head of water, which is flashing phenomenon.

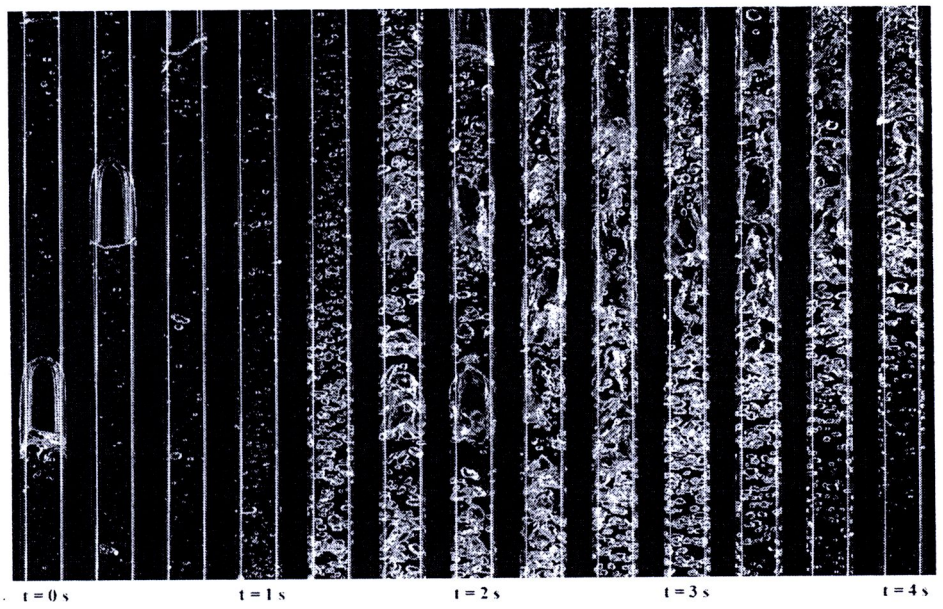

Fig. 5.16 Recorded bubble images at the riser middle

5.2.3 Spectrum analysis with FFT

The FFT was used to analyze the oscillation curve of the temperature and the differential pressure. At first, the frequency spectrum of the temperature oscillation at the heater outlet and the condenser outlet were presented. The frequency spectrum of the temperature oscillation at 8.0 kW/m^2 heat flux is shown in Fig. 5.17. The main frequency was found to be around 0.051 Hz for the temperature oscillation at the heater outlet, but there was no temperature oscillation observed at the condenser outlet. The frequency spectrum of the temperature oscillation at the heater outlet and at the condenser outlet for 12.5 and 18.0 kW/m^2 heat fluxes are shown in Fig. 5.18 and 5.19, respectively. At the heater outlet, the frequency of the temperature oscillation was found to be around 0.089 Hz for both heat fluxes. However, the spectrum became broadened with higher heat flux. The frequency of the temperature oscillation at the condenser

outlet increased from 0.01 to 0.014 Hz when heat flux increased from 12.5 to 18.0 kW/m^2. The frequency at the condenser outlet matched the low frequency component at the heater outlet. Therefore, the temperature oscillation at the heater outlet was a combined effect between the instability due to presence of the condenser and the flashing-induced density wave oscillation.

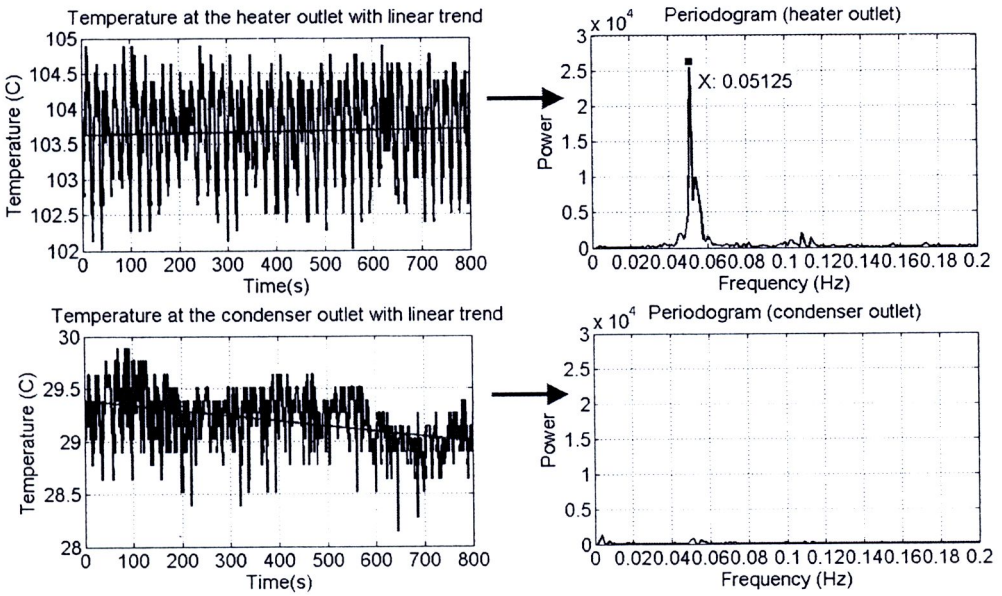

Fig. 5.17 FFT profiles of the temperature oscillation at the heater outlet and the condenser outlet for 8.0 kW/m^2 heat flux

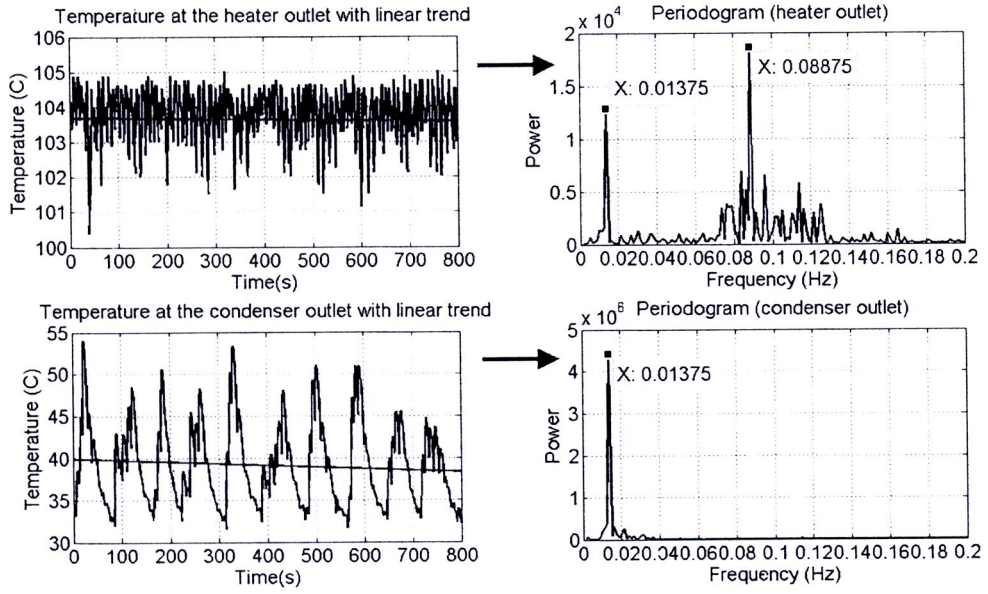

Fig. 5.18 FFT profiles of the temperature oscillation at the heater outlet and the condenser outlet for 12.5 kW/m^2 heat flux

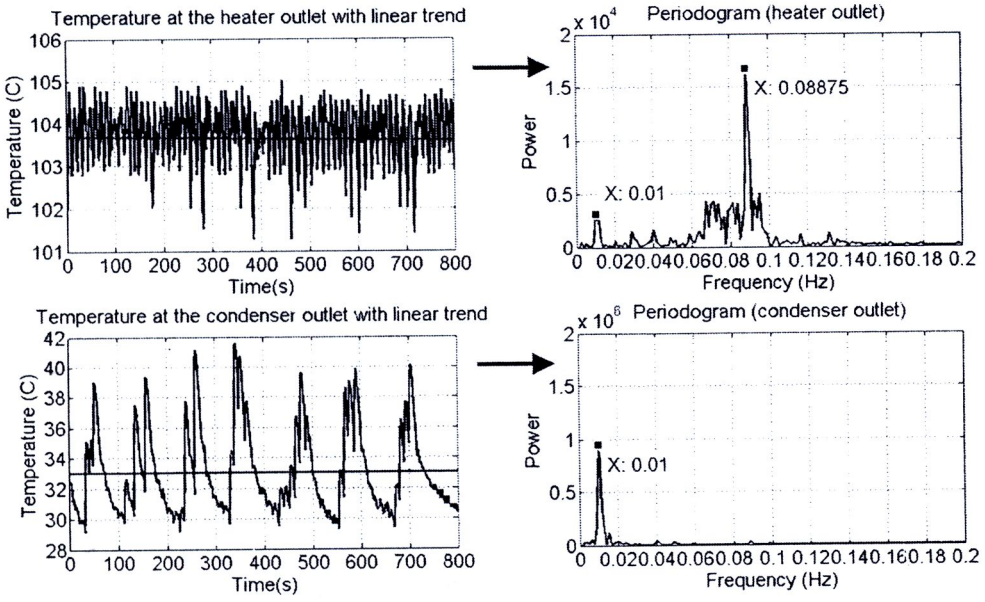

Fig. 5.19 FFT profiles of the temperature oscillation at the heater outlet and the condenser outlet for 18.0 kW/m^2 heat flux

For comparison, the frequency spectrums of the differential pressure oscillation at different heat fluxes were also analyzed. Fig. 5.20, 5.21, and 5.22 show FFT profiles of the differential pressure for 8.0, 12.5, and 18.0 kW/m^2 heat fluxes, respectively. It was found that the frequency of the differential pressure oscillation matched the frequency of the temperature oscillation at the heater outlet for each and every value of heat flux used. Therefore, it was concluded that the oscillations of both of differential pressure and the temperature at the heater outlet were driven by the boiling, which in turn was directly affected by the heat flux used in the experiment.

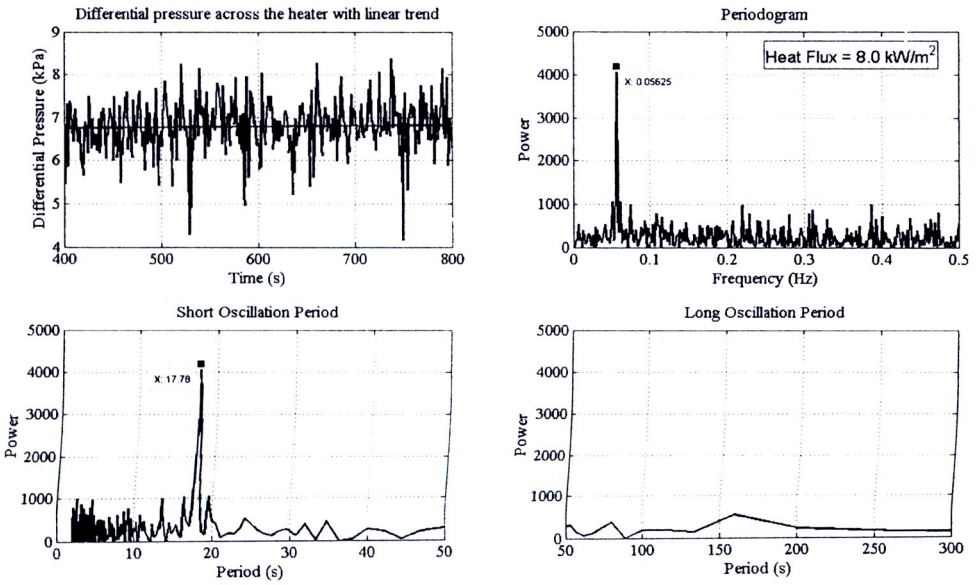

Fig. 5.20 FFT profiles of the differential pressure across the heater at 8.0 kW/m^2 heat flux

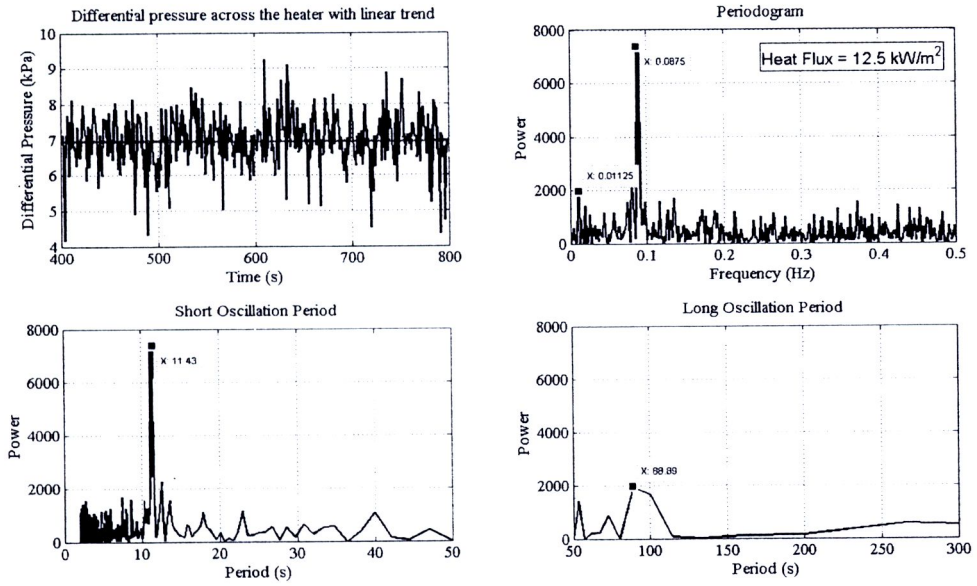

Fig. 5.21 FFT profiles of the differential pressure across the heater at 12.5 kW/m^2 heat flux

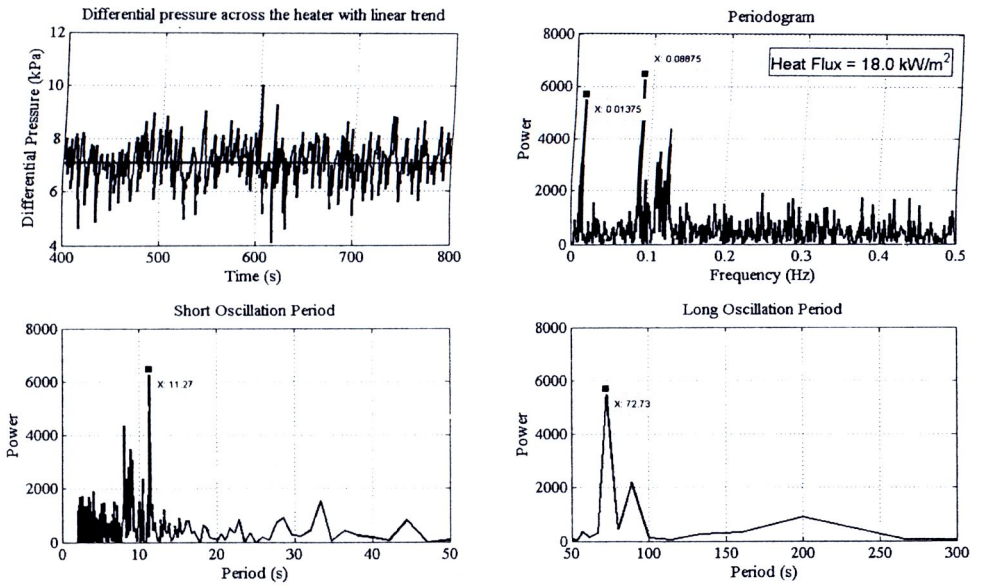

Fig. 5.22 FFT profiles of the differential pressure across the heater at 18.0 kW/m^2 heat flux

From the result of this work, the temperature oscillation of water in this configuration was due to flow instabilities which were known as geysering and flashing-induced density wave oscillation. FFT was a good method to analyze the oscillation curve when it became more complex.

5.3 The results from computer simulation

The TEXAS code was modified for simulation of a two-phase flow in the rectangular natural circulation loop as described in section 3.5. Fig. 5.23 shows a computer model for (a) the NCL#1 and (b) the NCL#2. The loop diameter is 22 mm. The loop height and width are 2000 mm and 1000 mm, respectively. The loop is divided into 60 meshes. Each mesh size is 100 mm long. The time step varies from 1 ns to 0.1 s. The initial conditions are shown in Table 5.1. The constant heat flux at heating section is used for heat input in the computer program.

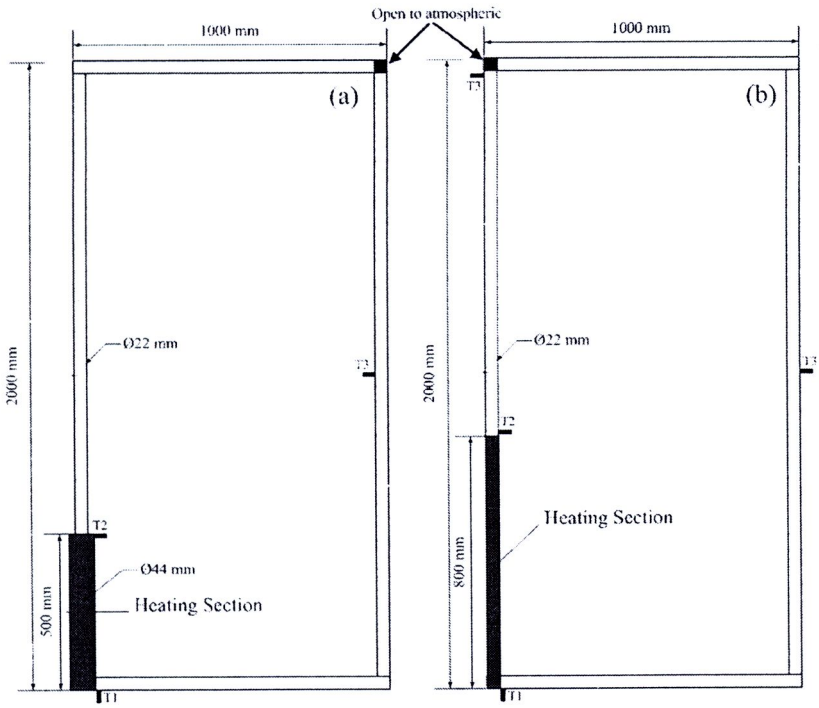

Fig. 5.23 A computer model for (a) the NCL#1 and (b) the NCL#2

Table 5.1 Initial conditions for computer simulation

Parameters	Value
System pressure (MPa)	0.1
Liquid and vapor velocity (m/s)	0
Liquid temperature (K)	303
Vapor temperature (K)	373
Wall temperature (K)	373
Void fraction	0

Fig. 5.24, 5.25, and 5.26 show the water temperature, liquid velocity, and pressure for the NCL#1, respectively. Liquid velocity in the tube diameter of 22 mm was higher than the tube diameter of 44 mm due to large cross section area. The pressure at the heater inlet was higher than the heater outlet due to pressure gradient in the loop. As shown in Fig. 5.26, the pressure initially fluctuated wildly before it was settled down. The fluctuation of pressure was due to build-up of pressure before initiated natural circulation.

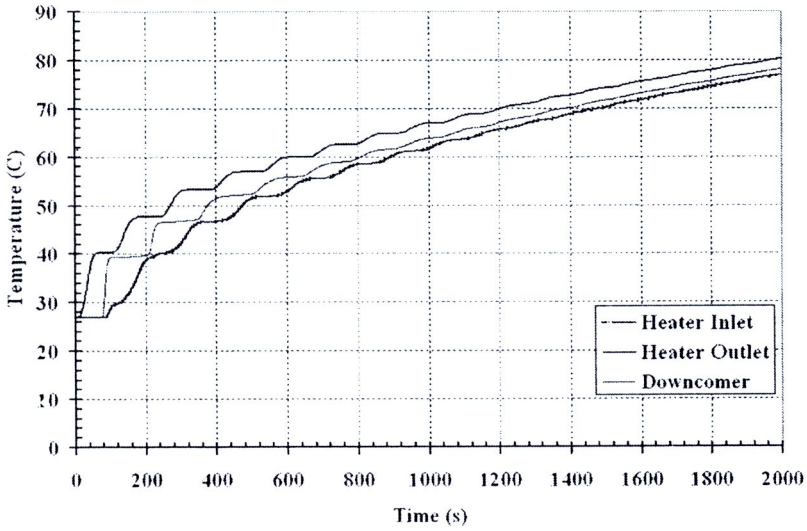

Fig. 5.24 Temperature profiles at 400 W heating powers

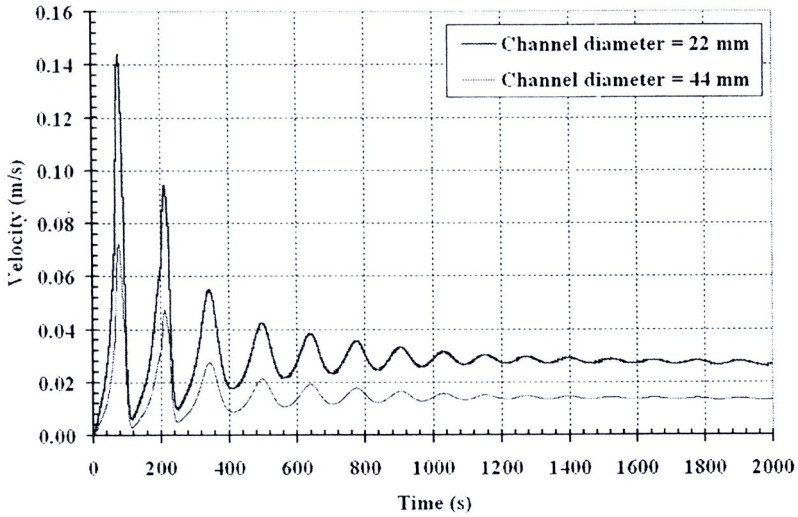

Fig. 5.25 Liquid velocity at 400 W heating powers

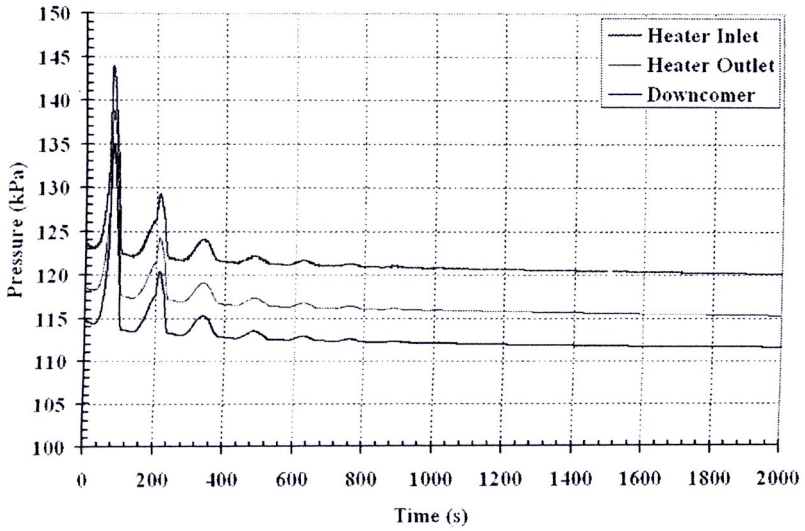

Fig. 5.26 Pressure at 400 W heating powers

Fig. 5.27 shows the water temperature at the heater outlet for the different heating power levels. It was found that at the same time, the water temperature was much higher when the heating power level was increased. The relationship between the water temperature and the water density is shown as Fig. 5.28. The water density was decreased with the increasing water temperature. This was indicated that equation of state for water in the computer program was correct.

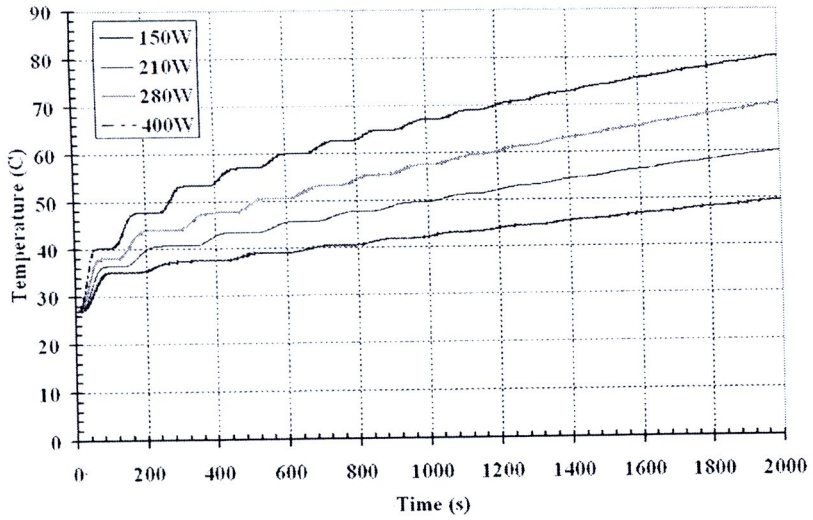

Fig. 5.27 The water temperature at various heating power levels

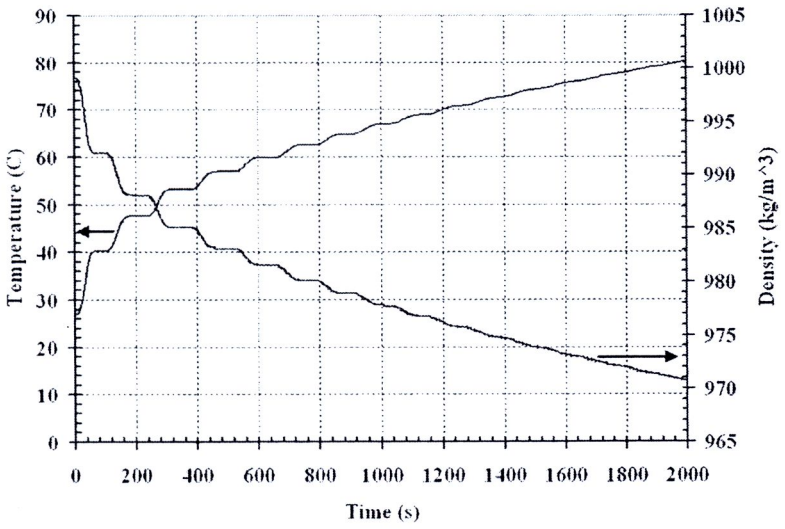

Fig. 5.28 The relationship between the water temperature and the water density

The water temperature oscillation was not observed in the computer simulation for 575 W heating powers as shown in Fig. 5.29. The differential pressure across the heater and the void fraction at the heater outlet for 575 W heating powers are shown in Fig. 5.30 and 5.31, respectively.

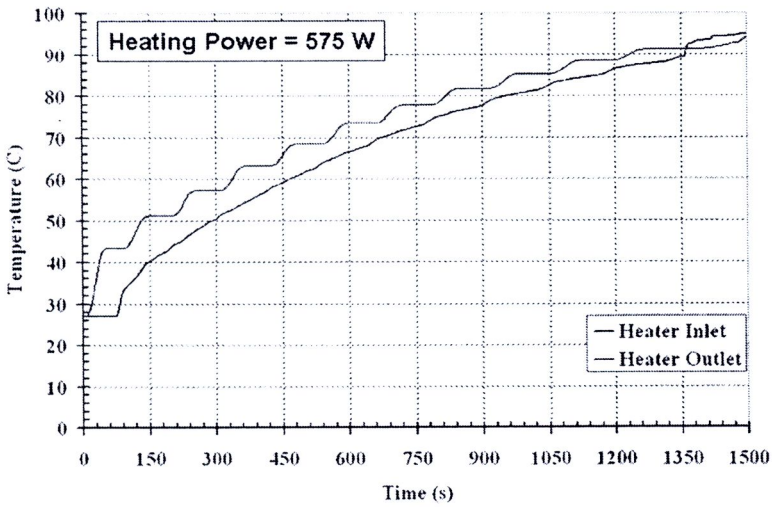

Fig. 5.29 Temperature profiles at 575 W heating powers

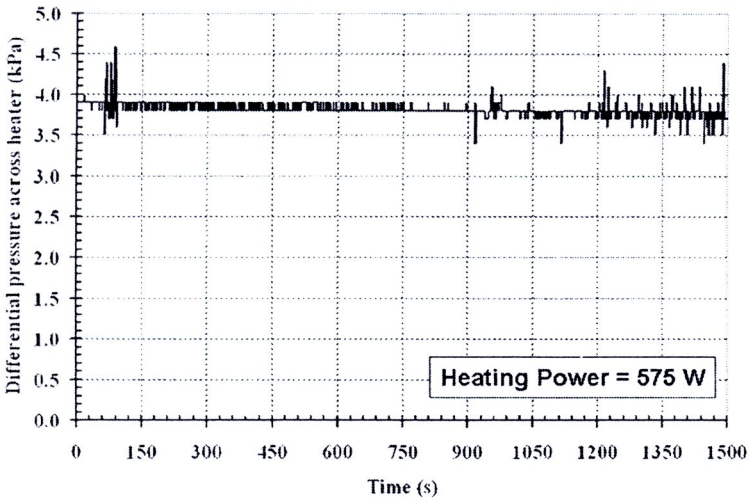

Fig. 5.30 Differential pressure across the heater at 575 W heating powers

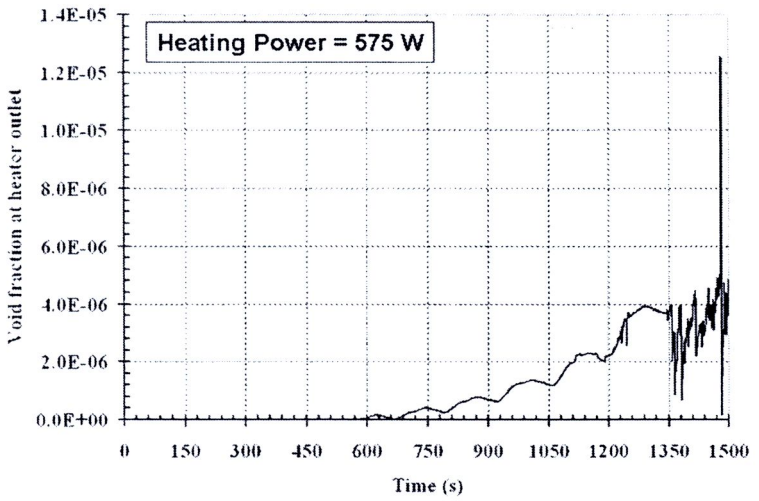

Fig. 5.31 Void fraction at the heater outlet at 575 W heating powers

Fig. 5.32, 5.33, and 5.34 show the water temperature, liquid velocity, and system pressure for the NCL#2. As shown in Fig. 5.33, the velocity initially fluctuated wildly before it was settled down. The fluctuation of velocity was due to large temperature difference along the loop at initiated flow. Again, the water temperature oscillation was not observed in the computer simulation for this loop.

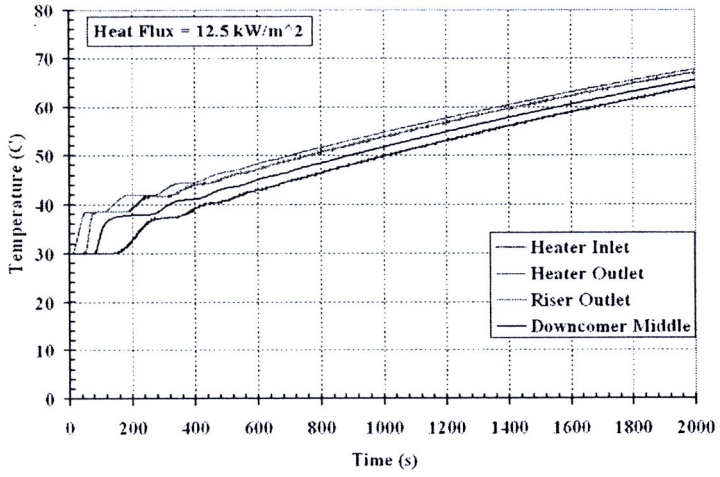

Fig. 5.32 Temperature profiles at 12.5 kW/m^2 heat fluxes

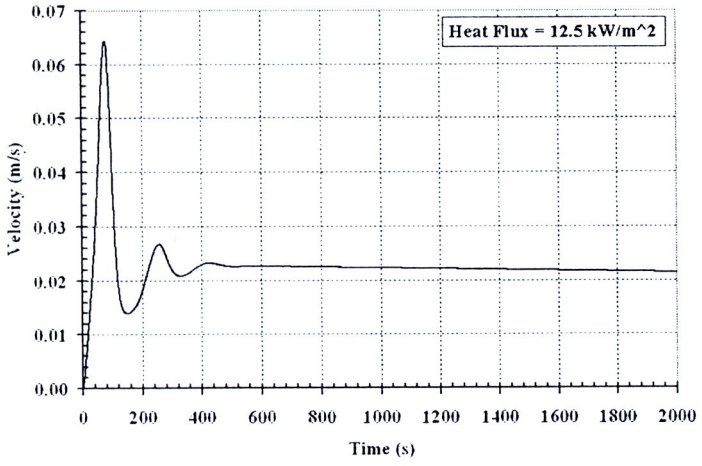

Fig. 5.33 Liquid velocity at 12.5 kW/m^2 heat fluxes

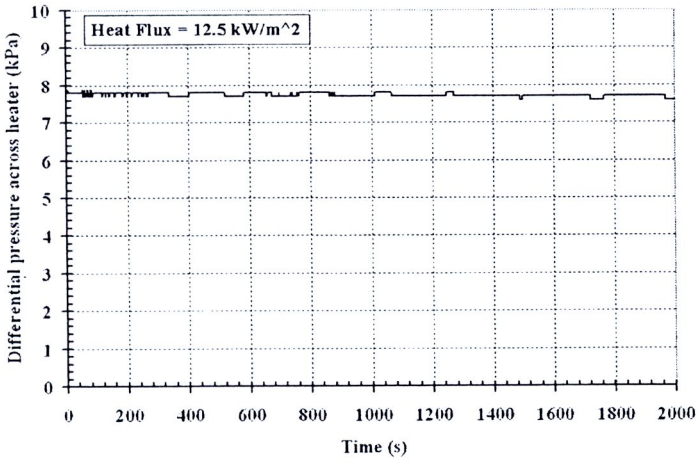

Fig. 5.34 Differential pressure across the heater at 12.5 kW/m^2 heat fluxes

5.4 Comparison of numerical and experimental results

Fig. 5.35-5.37 show the comparison of the numerical and experimental results. For the maximum temperature and the amplitude of initial fluctuation, the numerical results agree with the experimental results. However, the temperature difference across the heater is different from the experimental results. In addition, the water temperature oscillation was not observed in the computer simulation due to limitation of the computer program. Therefore, the computer program still required further modification.

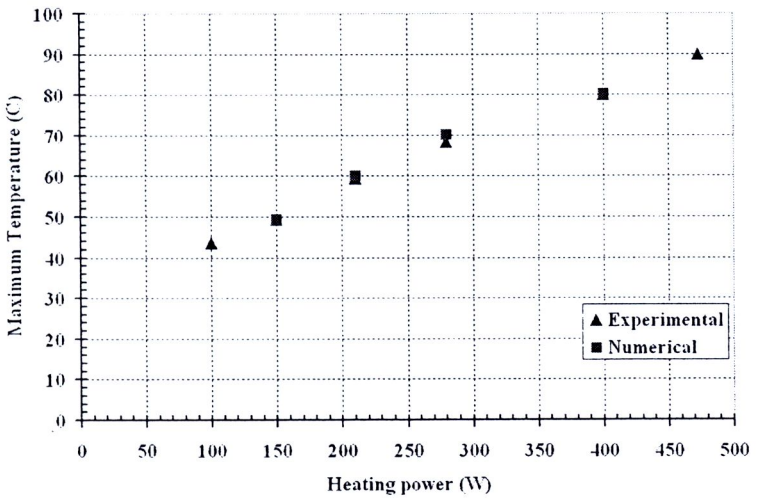

Fig. 5.35 Comparison of numerical and experimental results for the maximum water temperature

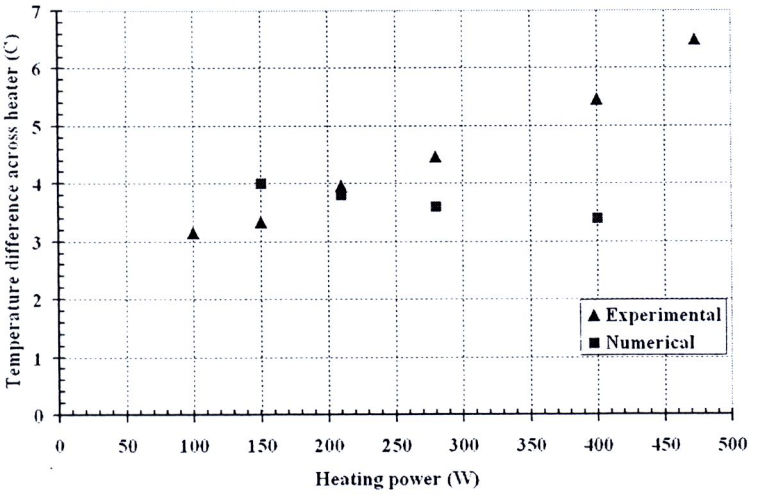

Fig. 5.36 Comparison of numerical and experimental results for the temperature difference across the heater

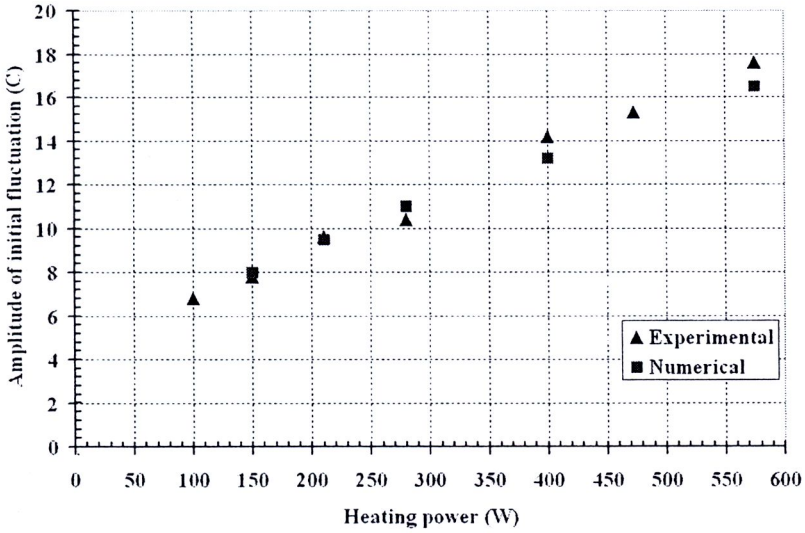

Fig. 5.37 Comparison of numerical and experimental results for the amplitude of initial fluctuation